JPMTR-2415
DOI 10.14622/JPMTR-2415
UDC 677.84:655.39:658.562:519.22:519.87:004.822 (045)

Original scientific paper | 197
Received: 2025-01-08
Accepted: 2025-04-17

Separating the effects of maximum pressure and printing nip length on flexographic print quality

Cecilia Rydefalk [1,2], Sofia Thorman [2], Anton Hagman [2] and Artem Kulachenko [1]

[1] Department of Engineering Mechanics,
KTH Royal Institute of Technology, Sweden
[2] Department of Sustainable Materials & Packaging,
RISE Research Institutes of Sweden, Sweden

rydefalk@kth.se

Abstract

When adjusting the impression in a printing press both the maximum pressure induced and the contact length between the print form and the substrate are simultaneously altered. In the present study, lab printing was performed with controlled load cases. The load cases were chosen to achieve varying nip lengths or maximum pressure. A lab-scale printing press was augmented with a pressure sensor that measures the width of the print over a square area. By altering the print forms and the force settings in the machine, the print nip pressure pulse was controlled. Printing was performed in both solid tone and halftone, and the printed result was evaluated for mottle, density, and dot-gain. By increasing the maximum pressure, the color density increases. By increasing the nip length at a fixed maximum pressure, the color density decreases. The variation within the settings in the present study is small and appears to originate from the split pattern. The change in the nip exit angle with increased nip length is sufficient to alter the ink split point and, thereby, the density. A higher maximum pressure can instead enable a higher ink transfer.

Keywords: flexography, lab printing, mottle, print density, ink transfer

1. Introduction

The assessment of print quality ranges from code legibility thresholds to fine-tuned image rendering aesthetics based on human perception. Tools to pinpoint and evaluate gloss, reflectance variations (mottle), tonal density, or uncovered areas (UCA) have been developed to put a number to the defects that disturb the visual appearance of a printed product. On the other hand, there are investigations into the mechanisms that induce wanted or unwanted effects and defects. In flexographic printing, there is a delicate interplay between the material properties of the substrate, the print plate, the foam backing, and the ink. Their individual stiffnesses, structure, wettability, and rheology add to that process parameters such as impression and print speed. The ink transfer from the print plate to the paperboard involves wetting of two solid surfaces with ink, one by the other, in a nip between two rolling cylinders. Upon exiting the nip, the fluid film splits between the plate and the substrate, whereupon the ink on the paperboard levels and sets. The visual appearance of the printed surface will depend on the thickness and uniformity of the ink layer. The amount of transferred ink depends on the ink available and where the film split occurs. Due to instabilities, the menisci at the nip exit will not be uniform but take on a wavy pattern. The cross machine direction (CD) wavelength depends on surface roughness, ink viscosity, and print speed (Brumm, Sauer and Dörsam, 2019). The liquid bridge between the print plate and the paperboard will stretch and rupture while the paperboard moves, which can create ink streak patterns in the machine direction (MD). The MD pattern is influenced by the elasticity of the ink (Morgan,, et al., 2018) and the asymmetry of the split that determines which surface will retain the larger amount of the ink. These finger-like patterns have even been specifically utilized to print biomimetic networks in a flexographic printer (Brumm,, et al., 2022). In packaging printing, this pattern is located in sub-millimetre wavelengths (Gil Barros, 2006) and is barely visible to the naked eye. Larger varieties, more noticeable to the eye, stem largely from structural variations of the paperboard.

Since contact is a requirement of ink transfer, the impression is one of the essential process parameters in

contact printing. If the impression is too low, the contact between the uneven paperboard and the print plate becomes insufficient to transfer ink. On the other hand, in flexography, a high impression can cause defects such as dot gain due to deformation of the raster dots. Too high impression in post-printing of corrugated board can crush the fluting (Holmvall, 2007). Printing with higher impressions can also cause the print plates to deteriorate faster.

It has been noted that optical density increases with impression (Tollenaar and Ernst, 1961) and that there is a significant improvement in density or tone value from engagement and during the initial increases in impression. However, at some point, an optimum impression is reached where further increasing of the impression provides none or minor increases in density (Bould, et al., 2011). Beyond the optimum impression, either the ink transfer has reached an equilibrium, or the ink transfer is still increasing, but the ink is forced into the paperboard coating. Using optical cross-section microscopy, Bohlin, Johansson and Lestelius (2016) concluded that a higher print force did not increase the penetration depth of the ink into the coating to any greater extent.

Several factors impact the liquid film split and the liquid distribution in meniscus rupture when stretching a liquid bridge. In the context of printing, this phenomenon has been studied most extensively with regard to gravure printing. It has been observed in studies regarding pick-out from a gravure cell that both shear and extension play an important part in the amount of fluid transferred, especially for non-Newtonian fluids (Khandavalli and Rothstein, 2017). The influence of ink elasticity on the split pattern compared to Newtonian ink was shown to alter the ribbing pattern in flexographic printing from straight lines to shorter structures in MD (Morgan, et al., 2018). Additionally, a difference in wettability between the two separating surfaces will affect the amount of liquid transferred between them. If the liquid being transferred is shear thinning, this has been found to enhance liquid transfer to the more wettable surface compared to the Newtonian case at the same capillary number (Wu, Carvalho and Kumar, 2019). Add to that the structure and surface energy of the paperboard, which will have its own effect on the ink spreading. A coated paperboard is often slightly hydrophobic due to the latex in the coating (Bohlin, Johansson and Lestelius, 2016). Applying pressure can mitigate the poor wettability (De Grace and Mangin, 1984). Forced wetting has even been shown to enable offset printing on a very hydrophobic Teflon surface (Liu and Shen, 2008).

Since the impression is an important parameter in the printing process, its isolated effect has been studied (Bohan, et al., 2003; Borbély and Szentgyörgyvölgyi, 2011). However, the impression is altered by closing the distance between the print cylinder and the impression cylinder, whereupon both the maximum pressure and the nip length will increase. The same applies to an increase in line load in a force-controlled lab press, both the maximum pressure and nip length is affected by the force setting. Additionally, the print plate, plate mounting sleeve or foam tape backing, and substrate are a combination of materials with a non-linear compression response. Additionally, all the materials can vary in thickness, and the resulting pressure pulse exerted on the substrate can both be asymmetric and change with print speed. The shape of the pressure pulse between two rolling cylinders, with or without deformable cover, has been extensively studied in the context of printing and other rolling processes (Hannah, 1951; Hunter, 1961; Bentall and Johnson, 1968; Margetson, 1971, 1972; Kerekes, 1976; Dobbels and Mewis, 1978; Watanabe and Amari, 1982; Coyle, 1988; Keller, 1992; Wang and Knothe, 1993; Xue, Gethin and Lim, 1994; Lim, et al., 1996; Luong and Lindem, 1997; Bohan, et al., 1997; Hinge and Maniatty, 1998; Yoneyama, Gotoh and Takashi, 2000; Johnson, 2003; Ascanio and Ruiz, 2006; Holmvall, 2007; Litvinov and Farnood, 2010; Austrell and Olsson, 2013; Abdel Rahman, El-Shafei and Mahmoud, 2014; Ceccato, Kulachenko and Barbier, 2019). Just to mention a few.

Many studies are numerical, or experiments confined to lab scale since measuring the pressure pulse in a full-scale printing press is difficult. However, Johnson, et al., (2004) measured the pressure pulse and ink transfer in a flexographic central impression printing press and showed that the nip length increased while the maximum pressure remained stable for an increased speed. They also measured the ink transfer in terms of copper content on the printed paperboard, showing that the amount of transferred ink decreased with increasing print speed. Something that had been previously noted in the literature for the optical density (Tollenaar and Ernst, 1961).

In the present study, we separate the maximum pressure from the nip length to study their separate effect on the print quality. The desired pressure pulses were achieved by altering the soft foam tape between the print plate and the cylinder and the force settings in the lab printer.

2. Material

2.1 Paperboard

The paperboard used in the present study was a multiply, coated, commercial liquid packaging paperboard. The mean local thickness (measured according to the method described by Schultz-Eklund, Fellers and Johansson (1992) was approximately 450 µm with a standard deviation of approximately 5 µm.

The grammage was 295 g/m^2. The surface roughness of the coated side (measured with an FRT MicroProf from Fries Research & Technology) had a standard deviation of approximately 3.3 µm around the mean surface height. The mean out-of-plane stiffness in compression was 23 MPa. The measurements on the paperboard were all performed in a climate-controlled laboratory (23 °C, 50 % RH) after conditioning the samples for 24 hours.

2.2 Printing plate

The printing plate was a photopolymer plate from XSYS. The plate was a 1.14 mm thick Xsys Nyloflex ACE with a hardness according to DIN 53505 of 62 and a Shore A of 78. The print plate had one solid tone area and one halftone area. The halftone was 30% on the printing plate (i.e., no dot gain compensation was applied) with a screen ruling of 48 lpi. The resulting print had roughly the same usable area of each.

2.3 Plate mounting foam tape

Three different plate mounting foam tapes were used to alter the pressure pulse. All three were from Lohmann and 0.5 mm thick. They are denoted 52, 53 and 54 with increasing stiffness.

2.4 Ink

The ink used was PremoNova WIPP-512N Cyan (FlintGroup).

3. Method

3.1 Print settings and resulting pulses

To print the samples in this study an IGT F1 laboratory flexographic printer was used. The printing speed was kept constant at 0.5 m/s. The speed is much lower than a full-scale printer. The lab printer is force-controlled and to evaluate the pressure pulses during printing a pressure sensor, Tekscan I-Scan 5040, was utilized. The setup was previously used and evaluated by Hedström (Hedström, 2023). The sensor is embedded in the sample holder and maps an area of 44 × 44 mm as it rolled through the nip together with a paperboard sample. A mean pulse has been calculated for each force setting used. The sensor was not present during printing, i.e. all the pressure measurements were performed during initial dry runs to determine the appropriate force settings for printing.

In Hedström's study, print plates of different thickness were used to achieve different pulses, but the conclusion was that the effect of changing the print plate overshadowed any other results. In the present study, only one print plate was utilized to ensure that the contact conditions between the plate and paperboard remained the same. The print force setting, and the foam tape were the only process parameters used to alter the pulse shape. Therefore, the resulting pulses could not achieve the large differences possible when using thin and hard plates and thicker, softer ones. The settings used in the present study are presented in Table 1 and the resulting mean pulses are shown in Figure 1. The pulses all have a unique force setting and will be denoted thereafter. As is marked in color in Table 1 and seen in Figure 1, some cases with different force settings achieve either the same max pressure or the same nip length. The relative change in nip length and maximum pressure are the same size; approximately 30 %. The testing was performed in a climate-controlled lab at standard climate (23 °C, 50 % RH).

In addition to the selected pulses, printing was performed at lower force settings, 20, 30 and 40 N, to evaluate if the optimum mottle and UCA had been reached.

3.2 Print evaluation

To evaluate the print quality in terms of mottle, density, reflectance, and tone value increase (TVI), all printed samples were scanned together with a reflectance calibration set at 600 dpi, RGB, in a flatbed scanner. One sample of each set was additionally scanned at 1200 dpi to evaluate dot reflectance, dot area, and the split

Table 1: Plate, tape, and print settings

Tape	Force setting [N]	Max pressure [kPa]	Nip length [mm]
Hard (54)	60	100	7
Medium (53)	70	100	8
Soft (52)	80	100	9
Soft (52)	125	150	10
Hard (54)	150	220	9
Medium (53)	175	220	10
Hard (54)	225	300	10

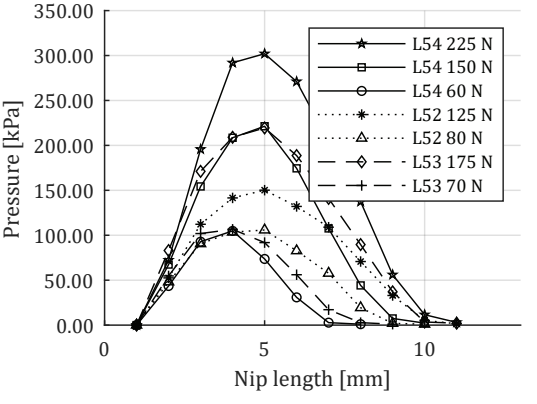

Figure 1: Pressure pulses during printing

pattern. The evaluation was performed using the software "STFI Mottle Expert" (RISE) (Christiansson, 2019) and "Dot Stat" (RISE)(described in a degree project of Kalicinski (2014).

3.2.1 Mean reflection, density and tone value increase

To calculate the mean (relative) density (Eq. [1]) and TVI (Eq. [2]), the red image channels of printed and unprinted areas calibrated to reflectance were used. The optical density presented is the relative density calculated from the calibrated reflectance of both the unprinted and printed surfaces. A decrease in reflectance from adding ink to the surface gives an increase in optical density.

$$\text{Relative Density} = \log_{10}\frac{\text{mean}\left(\text{Refl}_{\text{unprinted}}\right)}{100} - \log_{10}\frac{\text{mean}\left(\text{Refl}_{\text{printed}}\right)}{100} \quad [1]$$

The TVI is calculated against the relative density and the nominal tone value of the print plate using the Murray–Davies equation.

$$\text{TVI} = \frac{1-10^{-\text{RelDensity}_{\text{halftone}}}}{1-10^{-\text{RelDensity}_{\text{solid tone}}}} \cdot 100 - \text{nominal tone} \quad [2]$$

The TVI does not distinguish between physical and optical dot gain. The mean TVI information is augmented by analyzing the dot area and dot reflectance.

3.2.2 Mottle and uncovered areas

The mottle and UCA are calculated from grey-scale images calibrated to reflection. In the solid tone areas, the threshold for detecting UCA was 13 % above the mean reflectance. The feature in STFI-Mottling Expert called "Remove false UCA" was used. Areas larger than 500 mm^2 and fiber shaped areas with a reflectance above thresholds of 13 % above the mean reflectance were considered false UCA. The areas were replaced with the mean reflectance of their surroundings. The mottle is given as the coefficient of variation of the reflectance. The information is filtered and is divided into the following wavelength spans: 0.13–0.25, 0.25–0.5, 0,5–1, 1–2, 2–4, 4–8 and 1–8 mm.

4. Results

Several print quality metrics were utilized to evaluate the effect of the maximum pressure and nip length. All error bars represent 95 % confidence interval.

4.1 Optimum plateau for uncovered areas and mottle

Both the UCA and the detected false UCA decrease with increasing force setting, as shown in Figure 2. This is expected when the plate-paperboard contact increases. At the lower end of the settings, the software has discovered some false UCA's, which might be actual UCA's since they appear more prevalent in low-pressure cases. However, for the selected range of settings, both UCA and false UCA have plateaued near to or at zero.

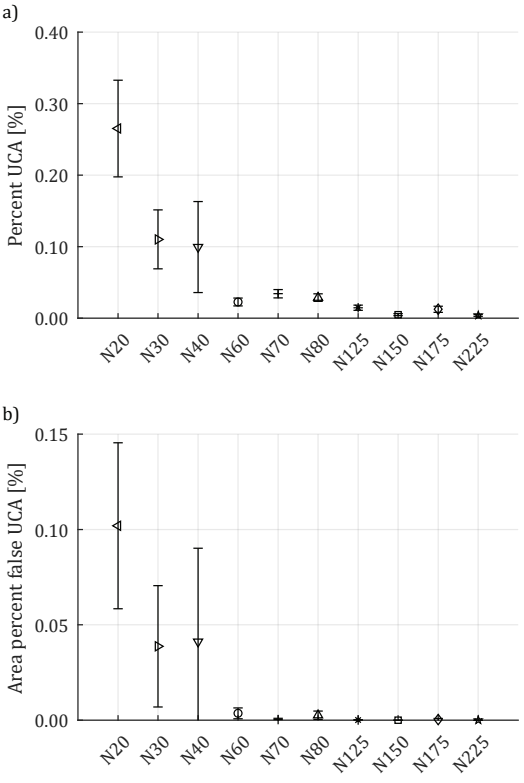

Figure 2: Uncovered areas (a) and false uncovered areas (b)

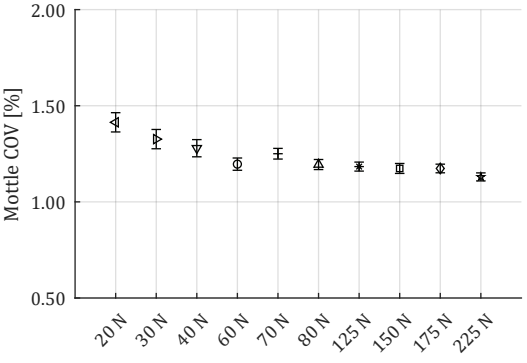

Figure 3: Solid tone mottle 1–8 mm. COV denotes the uncovered areas

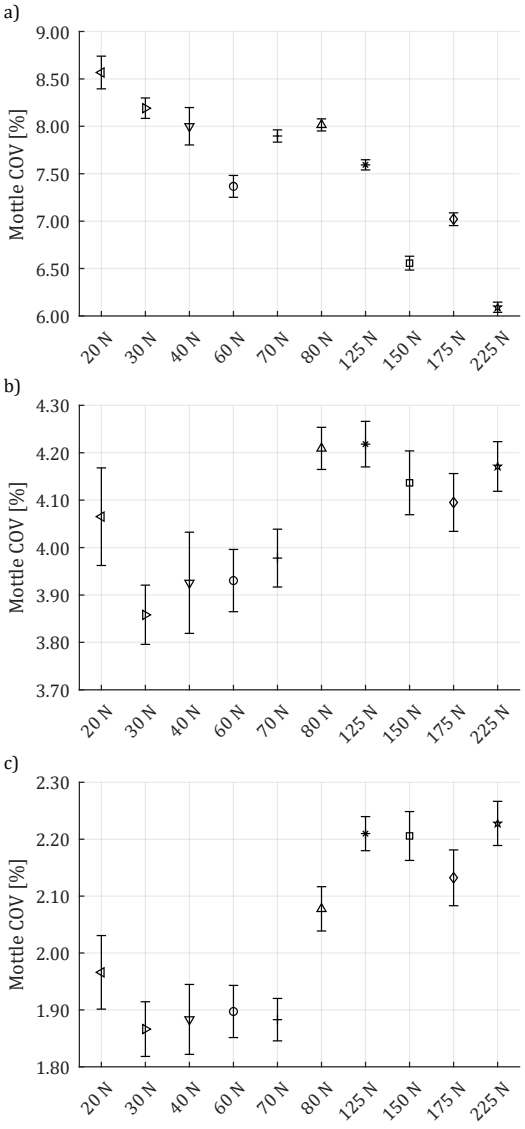

Figure 4: Solid tone mottle

In Figure 3 the 1–8 mm mottle in the solid tone is presented. For a set combination of plate and paperboard, the increased impression will improve the 1–8 mm mottle until it plateaus. As can be seen in Figure 3 the plateau is reached for the selected settings. However, it should be noted in Figure 4 that although the 1–8 mm mottle plateaus, it keeps improving in the 0.13–0.25 mm wavelengths. Additionally, in 0.25–1 mm there is a jump between 70 N and 80 N.

4.2 Solid tone reflectance and density

The solid tone reflectance scans are shown Figure 5 and the values are presented in Figure 6. Using Equation [1] the density is calculated and presented in Figure 7. Increasing the maximum pressure while keeping the nip length constant reduces the reflectance and thereby increases the density. However, increasing the nip length while maintaining the same maximum pressure increases the reflectance and decreases the density. The density range for all the cases presented here is, however, within acceptable boundaries for a full-scale print run.

4.3 Halftone reflectance and density

The halftone reflectance and density are shown in Figure 9 and Figure 9. The halftone follows the same trend was observed in the solid tone in Figure 6 and Figure 7. The effect is slightly larger in the halftone compared to the solid tone, especially for the higher forces, which could be explained by an expanded dot area at higher impressions. The dots are more easily deformed than the solid surfaces on the print plate. Additionally, in the halftone, the line load is distributed over a surface that is 30 % of the solid tone area.

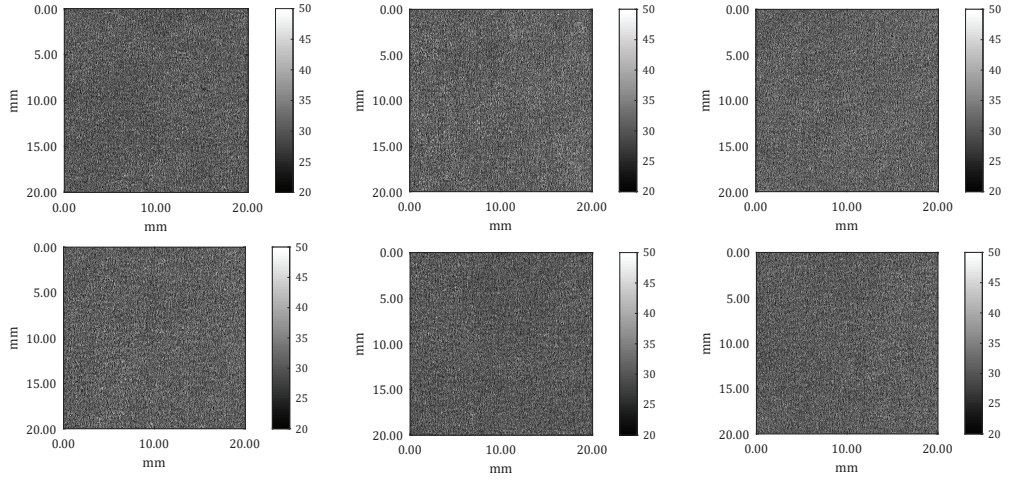

Figure 5: Calibrated reflectance patterns 20 × 20 mm

4.4 Dot area, dot reflectance and tone value increase

The TVI in the halftone is calculated according to Equation [2] and presented in Figure 10. It follows the same trend as the density in both the solid and halftone (Figures 7 and 9, respectively). The TVI is expected to increase with increased pressure due to the mechanical deformation of the dots and squeeze out of the ink at the rim of the dots. However, the fact that the dot gain decreases with nip length at a fixed maximum is surprising and indicates a different mechanism in the ink transfer.

The TVI presents a value for the entire printed surface but does not account for if the TVI is caused by larger and/or darker dots. Therefore, the reflectance of the individual dots was analyzed from the higher resolution scans and were presented in Figure 11. The reflectance of the individual dots follows the same pattern as the solid tone reflectance. However, the results show that the area of the dots are also affected. A longer nip at the same maximum pressure produces smaller and slightly lighter dots. An increased maximum pressure with maintained nip width creates larger, darker dots. This indicates that the halftone density of the whole area in

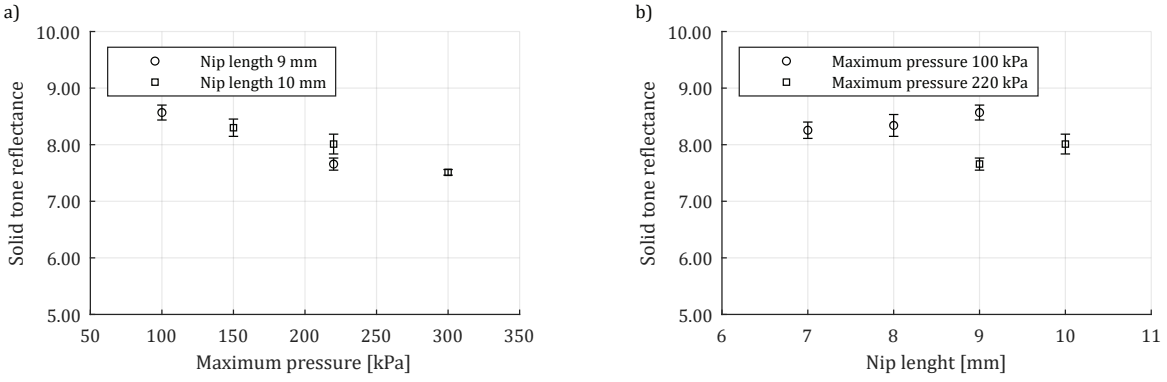

Figure 6: Solid tone reflectance versus maximum pressure (a) and nip lengt (b)

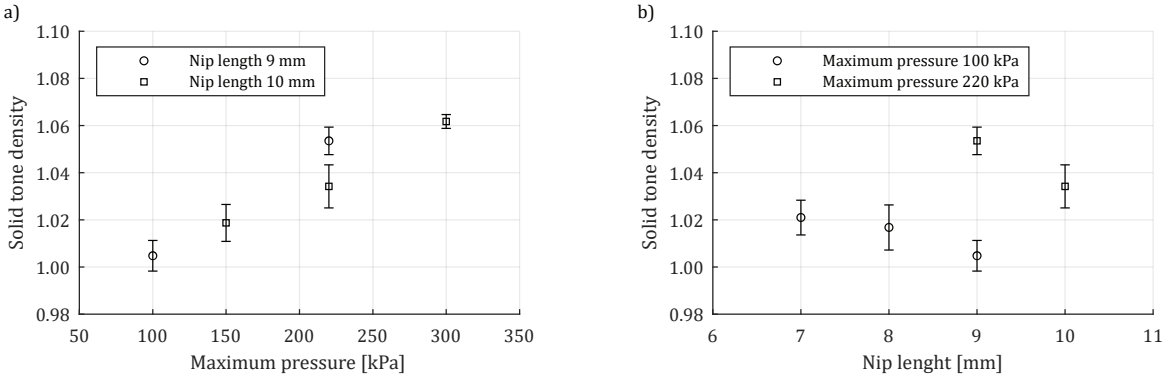

Figure 7: Solid tone density versus maximum pressure (a) and nip lengt (b)

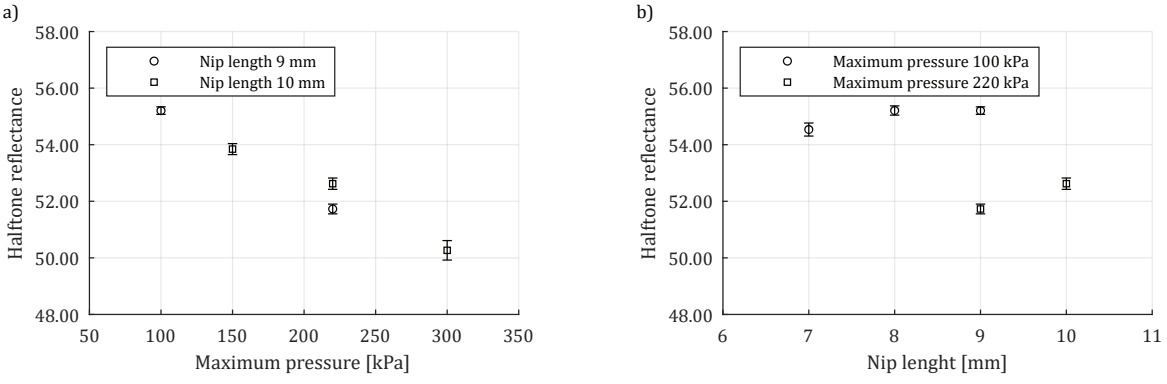

Figure 8: Halftone reflectance versus maximum pressure (a) and nip length (b)

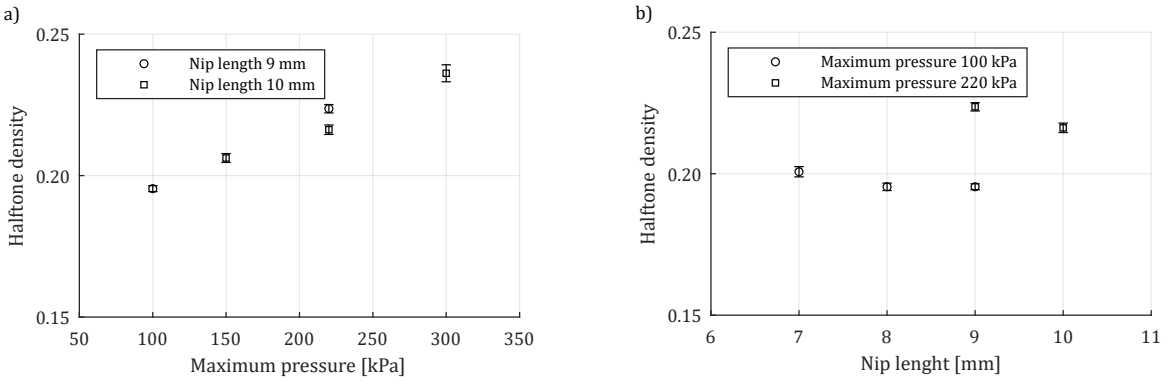

Figure 9: Halftone density versus maximum pressure (a) and nip length (b)

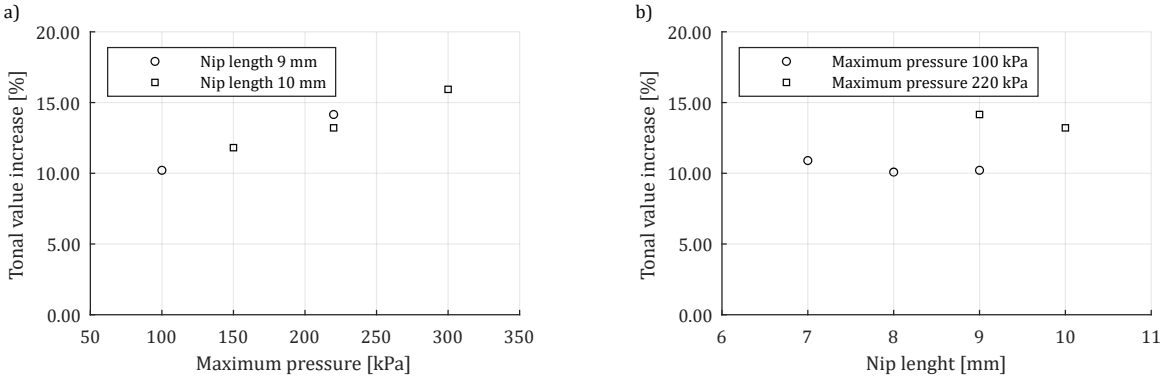

Figure 10 Dot gain (% increase from nominal tone value) versus maximum pressure (a) and nip lenght (b)

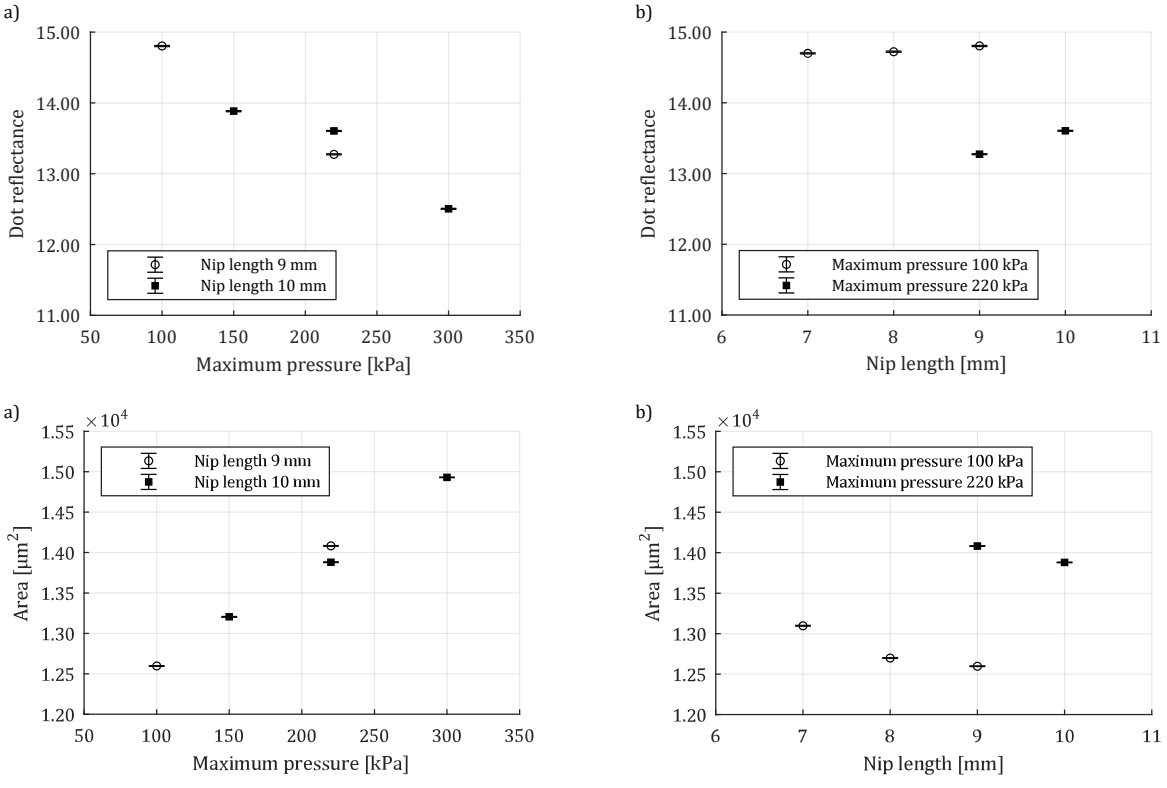

Figure 11: Dot reflectance and area versus maximum pressure (a) and nip length (b)

Figure 9 and the TVI in Figure 10 are due to a change in both the area and reflectance of the individual dots. Less ink appears to have been transferred when the nip length is extended at the same maximum pressure in the dots as well as in the solid tone.

4.5 Print mottle and ink splitting pattern

The solid tone mottle is presented (one wavelength span per subplot) in Figure 12 (plotted against the maximum pressure) and in Figure 13 (plotted against the nip length). There is a very slight improvement in 1–8 mm when the maximum pressure is increased. The shortest wavelength, 0.13–0.25 mm, displays the most noticeable improvement in mottle when the maximum pressure is increased. However, when increasing the nip length at the same pressure the mottle increases. The same trend as seen in the reflectance in Figure 6 is seen here in Figure 13 in the reflectance variation (mottle) in 0.13–0.25 mm. This wavelength is where the split pattern can be found (Gil

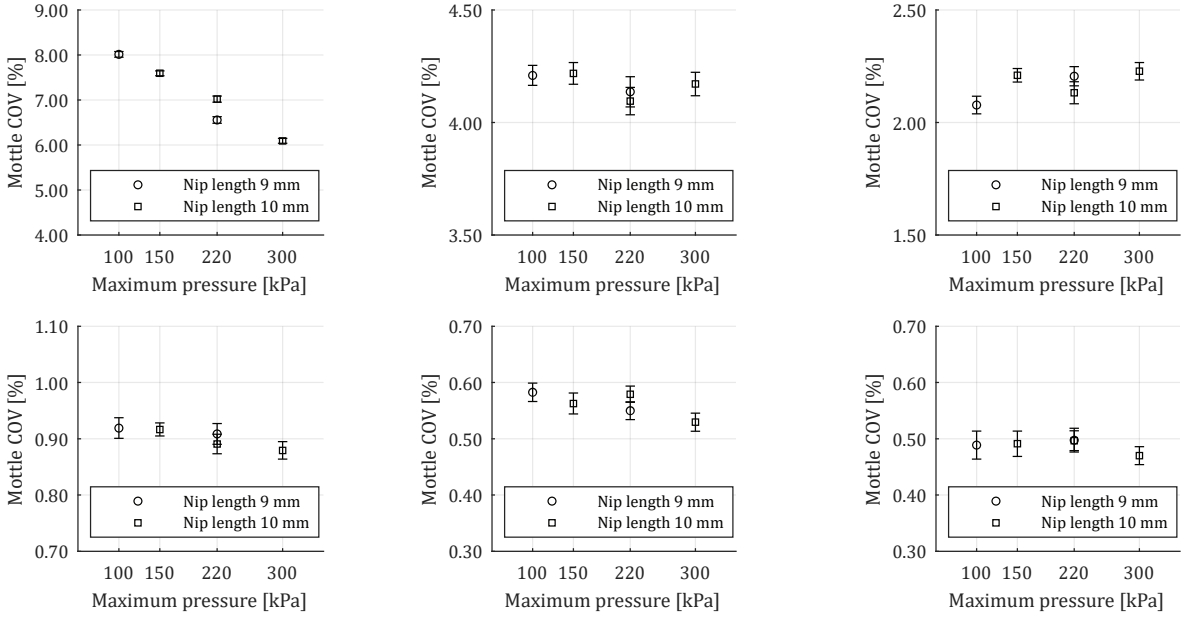

Figure 12: Solid tone mottle versus maximum pressure per wavelength span (COV)

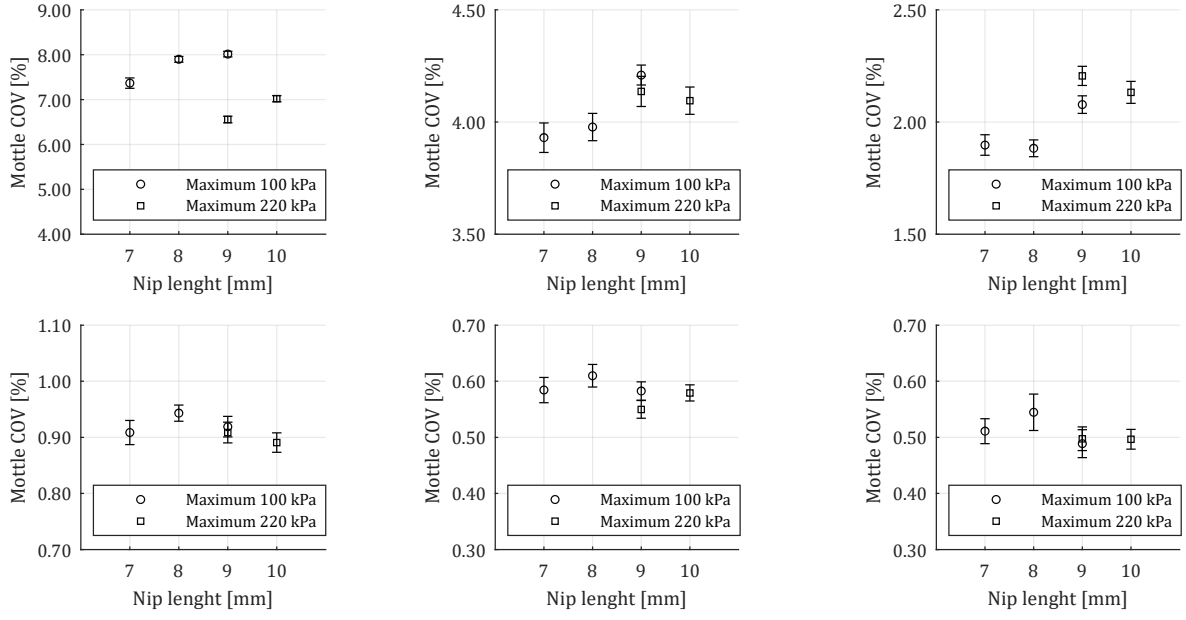

Figure 13: Solid tone mottle versus nip length per wavelength span (COV)

Barros, 2006). Even if the split pattern is similar for the different settings, the variation in the smallest wavelength could indicate how much ink is in the liquid bridge on the paperboard side when it ruptures.

The split patterns are visible in the plots of the calibrated reflectance in Figure 5. A closer look at the local ink density is visualized in Figure 14 where the data has been interpolated in MATLAB to make the gradients smoother. The split pattern is formed by the ribbing instability of the moving contact line and the liquid filament or bridge between the plate and paperboard that breaks and leaves small-scale dots or streaks in the machine direction on the substrate. The patterns show no obvious differences, but there are reflectance variations in 0.125–0.3 mm shown in Figures 12 and 13. The mottle trend in this wavelength span follows the reflectance difference between the settings. A decrease in reflectance means an increase in density, thus indicating that there is a small change in the split point. On one hand, increasing the density and reducing the variation in the shortest wavelength with increasing maximum pressure, and on the other hand, decreasing the density and slightly increasing the variation when the nip length is extended were observed.

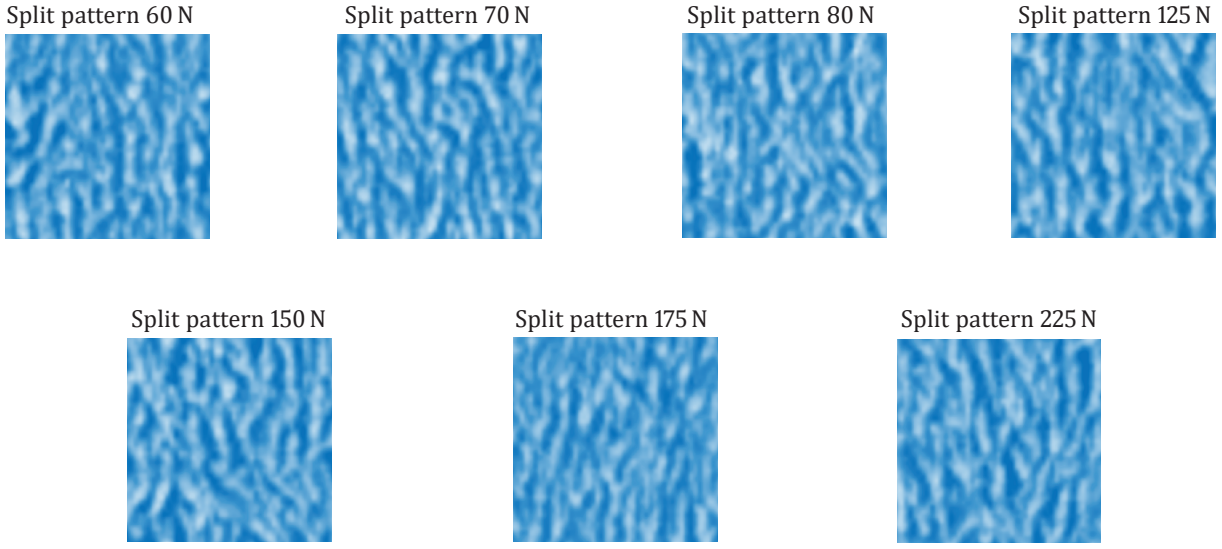

Figure 14: Visualization of the local ink density showing the split pattern

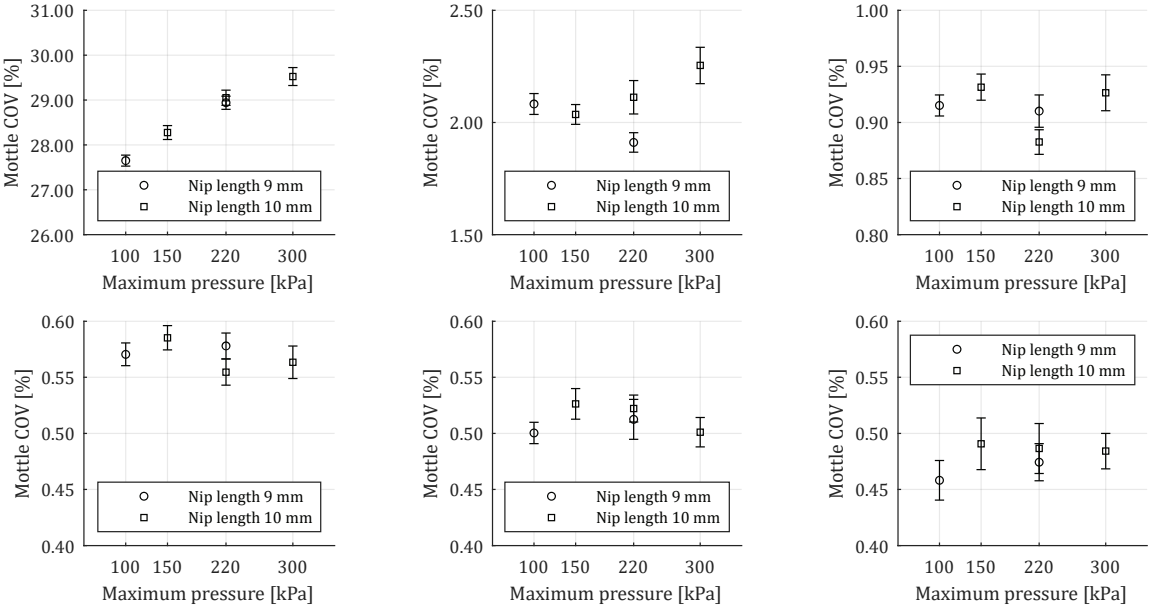

Figure 15: Halftone mottle vs. maximum pressure per wavelength span [COV]

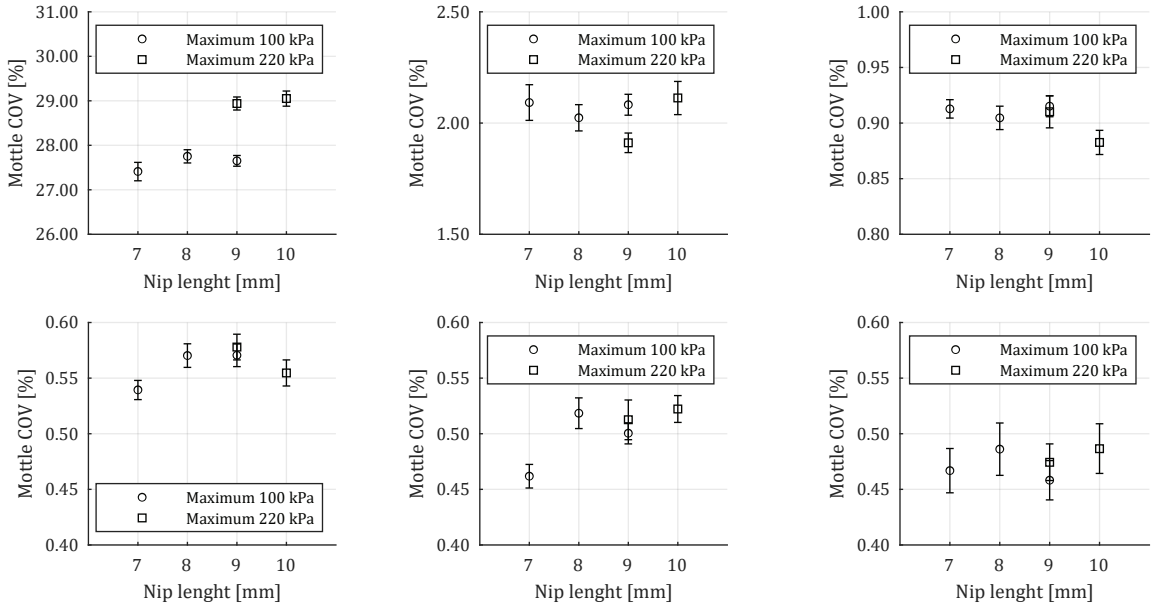

Figure 16: Halftone mottle vs. nip length per wavelength span [COV]

The halftone mottle is presented in Figures 15 and 16. The wavelength 0.13–0.25 mm is heavily influenced by the dot pattern due to the dot size in the halftone. The largest variation between the cases occurs in the shortest wavelengths, 0.25–0.5 mm. In the middle span, 1–4 mm, only the lowest force setting sticks out with a lower value. At the longest wavelengths, 4–8 mm, there is a large variation in all force settings but no significant difference between the settings.

5. Discussion

The result that the UCA's decreased with print force was expected, as well as the stabilization of print mottle in the higher wavelengths. However, the reduced solid tone density with nip length was one unexpected result. Another unexpected result was that the density of the dots as well as their area also decreased with a longer nip length at the same maximum pressure.

The optical density alone cannot completely rule out the possibility of another mechanism that could "hide" the ink, making the surface appear lighter compared to how much ink was transferred. However, Bohlin, Johansson and Lestelius (2016) concluded using optical cross-section microscopy that an increased force did not make the ink penetrate deeper into the substrate to any greater extent. Additionally, the halftone density can be affected by effects such as optical dot gain. As the substrate was the same in all cases, we assume that the optical dot gain remains on a similar level and that the halftone density differences are mostly a result of the actual differences in ink transfer. Another way to measure the ink transfer is to measure the copper content on the paperboard using Atomic Absorption Spectroscopy, AAS. This will provide an amount of g/m^2 of dry ink, regardless of the optical qualities of the print. A study of the pressure pulse and ink transfer at different speeds has been performed by Johnson, et al. (2004). In the paper, they show that for the hard flexographic print plate (comparable to the one used in the present study), the increase in speed resulted in a longer nip, unchanged maximum pressure, and a decrease in g/m^2 of ink transferred. With consistent maximum pressure and increasing nip length, we observe a decrease in density just as they observe a decrease in ink transfer. We therefore assume that the decrease in optical density is due to less ink transferred. In Johnson's study, the speed was increased (and the ink transfer decreased), while in this study, the print speed in the IGT F1 was kept constant. In their study they could not rule out that the shortened duration (time) in the nip was the cause of the decrease in ink transfer. However, in both studies, the nip length was increased with a maintained maximum pressure.

An increase in nip length (for the same print cylinder) will result in a more acute exit angle and a larger vertical velocity component. It had previously been observed that an increase in print speed in the lab printer affected the split pattern, therefore the print speed was held constant in this study. The same print plate was used to ensure that the paperboard–print plate contact remained the same. The paperboard samples came from the same reel, and although the wettability of the paperboard and print plate are unknown, their relationship should remain unchanged within the present print run. However, the nip exit will change with the nip length.

At the nip exit the split point of the filaments between paperboard and print plate will influence the amount of ink transferred. And a pair of results that followed each other was the solid tone reflectance and the mottle in the shortest wavelength. The mottle that corresponds to the split pattern. The nip exit exhibits a complex load case. The fluid is both extended with the lifting print plate, but it is also sheared due to the moving paperboard. The extension also includes a rotation and acceleration of the print plate. It is therefore not necessarily sufficient to only consider the extensional rheology or shear of ink. Dodds, Carvalho and Kumar (2012) studied the behavior of a bridge of Newtonian fluid stretched under both extension and rotation in the context of gravure printing. The study concluded that the acceleration of one plate relative to the other has a significant effect on the bridge dynamics and the transfer of liquid. They commented that the implication is that by producing a difference in rotation of one surface against the other, the amount of liquid transferred can be slightly altered. In gravure printing, they noted, this could be performed by a mismatch in the size of the two rolls. In our case, by altering the angle at the split, the amount of ink transferred is slightly altered. This mechanism could explain why the density decreases with increasing nip length. The other mechanism working in the opposite direction is the maximum pressure. With an increase in maximum at the same nip length (and therefore exit angle conditions), more ink was transferred to the paperboard. At lower impressions or force settings the print is improved by increasing the pressure, establishing better contact, and reducing UCA and mottle towards their optimum. However, the printing was performed after reaching the plateau. The mechanism could be related to forced absorption of the liquid part of the ink due to the higher pressure while the pigments remain at the surface. It could also be an effect of forced wetting due to the increase pressure, thereby increasing the adhesion of the ink on the paperboard.

6. Conclusions

The velocity and exit angle differences in the nip exit are sufficient to alter the point of meniscus rupture so that the ink transfer becomes smaller with the longer nip. The mechanism that governs the effect of increasing the maximum remains unexplained but is in line with previous studies and observation. However, the combined result could help explain why an increase in speed requires an increase in impression. If the nip length is altered, there is more than just the shorter duration that could affect the ink transfer. The nip exit effect on the split point plays a role too. An increased pressure mitigates the effect of the longer nip length. However, both the area and the reflectance of the dots were affected by the settings and the longer nip length slightly reduced the tone value increase.

7. Acknowledgments

Anton Hedström's work during his degree project (2023) is greatly appreciated and was the basis for the present study. Without his evaluations of the setup and the scripts he wrote, the present study would not have been possible within the scope of the present project.

References

Abdel Rahman, A.A., El-Shafei, A.G. and Mahmoud, F.F. (2014) 'Nonlinear analysis of viscoelastically layered rolls in steady state rolling contact', *International Journal of Applied Mechanics*, 6(6), 1450065. Available at: https://doi.org/10.1142/S1758825114500653.

Ascanio, G. and Ruiz, G. (2006) 'Measurement of pressure distribution in a deformable nip of counter-rotating rolls', *Measurement Science and Technology*, 17(9), pp. 2341–2346. Available at: https://doi.org/10.1088/0957-0233/17/9/009.

Austrell, P.E. and Olsson, A.K. (2013) 'Modelling procedures and properties of rubber in rolling contact', *Polymer Testing*, 32(2), pp. 306–312. Available at: https://doi.org/10.1016/j.polymertesting.2012.11.015.

Bentall, R.H. and Johnson, K.L. (1968) 'An elastic strip in plane rolling contact', *International Journal of Mechanical Sciences*, 10(8), pp. 637–663. Available at: https://doi.org/10.1016/0020-7403(68)90070-2.

Bohan, M.F.J., Lim, C.H., Korochkina, T.V., Claypole, T.C., Gethin, D.T., Roylance, B.J. (1997) 'An investigation of the hydrodynamic and mechanical behaviour of a soft nip rolling contact', Proceedings of the Institution of Mechanical Engineers, Part J: *Journal of Engineering Tribology*, 211(1), pp. 37–49. Available at: https://doi.org/10.1243/1350650971542309.

Bohan, M.F.J., Hamblyen, S., Claypole, T., Gethin, D.T. (2003) 'Evaluation of pressures in flexographic printing', in *Proceedings of the Technical Association of the Graphic Arts*, TAGA, pp. 311–320. Available at: https://www.researchgate.net/profile/Tim-Claypole-2/publication/265409485_Evaluation_of_Pressures_in_Flexographic_Printing/links/54ccbb2a0cf298d6565ac1fa/Evaluation-of-Pressures-in-Flexographic-Printing.pdf (Accessed: 3 April 2024).

Bohlin, E., Johansson, C. and Lestelius, M. (2016) 'Flexographic ink-coating interactions: Effects of latex variations in coating layers', *Tappi Journal*, 15(4), pp. 253–262. Available at: https://doi.org/10.32964/tj15.4.253.

Borbély, Á. and Szentgyörgyvölgyi, R. (2011) 'Colorimetric properties of flexographic printed foils: the effect of impression', *Óbuda University e-Bulletin*, 2(1), pp. 2011–2042. Available at: https://oda.uni-obuda.hu/bitstream/handle/20.500.14044/25205/21902_BorbelyAkos_Szentgyorgyvolgyi_2.pdf (Accessed: 19 July 2024).

Bould, D.C., Hamblyn, S.M., Claypole, T., Gethin, D.T. (2011) 'Effect of impression pressure and anilox specification on solid and halftone density', *Journal of Engineering Manufacture*, 225(5), pp. 699–709. Available at: https://doi.org/10.1177/2041297510394072.

Brumm, P., Fritschen, A., Doß, L, Dörsam, E., Blaeser, A. (2022) 'Fabrication of biomimetic networks using viscous fingering in flexographic printing', *Biomedical Materials*, 17(4), p. 045012. Available at: https://doi.org/10.1088/1748-605X/AC6B06.

Brumm, P., Sauer, H.M. and Dörsam, E. (2019) 'Scaling behavior of pattern formation in the flexographic ink splitting process', *Colloids and Interfaces*, 3(1), 37. Available at: https://doi.org/10.3390/COLLOIDS3010037.

Ceccato, C., Kulachenko, A. and Barbier, C. (2019) 'Investigation of rolling contact between metal and rubber-covered cylinders governing the paper compaction process', *International Journal of Mechanical Sciences*, 163, p. 105156. Available at: https://doi.org/10.1016/J.IJMECSCI.2019.105156.

Christiansson, H. (2019) *STFI-Mottling Expert 1.37*. RISE Research Institutes of Sweden.

Coyle, D.J. (1988) 'Forward roll coating with deformable rolls: A simple one-dimensional elastohydrodynamic model', *Chemical Engineering Science*, 43(10), pp. 2673–2684. Available at: https://doi.org/10.1016/0009-2509(88)80011-3.

Dobbels, F. and Mewis, J. (1978) 'Analysis of nip flow operations involving a viscoelastic roller', *Chemical Engineering Science*, 33(4), pp. 493–500.

Dodds, S., Carvalho, M.S. and Kumar, S. (2012) 'The dynamics of three-dimensional liquid bridges with pinned and moving contact lines', *Journal of Fluid Mechanics*, 707, pp. 521–540. Available at: https://doi.org/10.1017/JFM.2012.296.

De Grace, J. H. and Mangin, P. J. (1984) 'A mechanistic approach to ink transfer. Part I: Effects of substrate properties and press conditions', in W. H. Banks (ed.) Advances in Printing Science and Technology, pp. 312–332. London: Pentech Press.

Gil Barros, G. (2006) *Influence of Substrate Topography on Ink Distribution in Flexography.* Doctoral dissertation. Karlstads universitet. Available at: https://urn.kb.se/resolve?urn=urn:nbn:se:kau:diva-446 (Accessed: 27 June 2024).

Hannah, M. (1951) 'Contact stress and deformation in a thin elastic layer', *The Quarterly Journal of Mechanics and Applied Mathematics*, 4(1), pp. 94–105. Available at: https://doi.org/10.1093/QJMAM/4.1.94.

Hedström, A. (2023) *Evaluating the Pressure Pulse in a Flexographic Printing Press: Linking Process Parameters to specific Pulse Shapes*. Master thesis. KTH Royal Institute of Technology, Stockholm. Available at: https://urn.kb.se/resolve?urn=urn:nbn:se:kth:diva-325081 (Accessed: 15 July 2024).

Hinge, K.C. and Maniatty, A.M. (1998) 'Model of steady rolling contact between layered rolls with thin media in the nip', *Engineering Computations* (Swansea, Wales), 15(6–7), pp. 956–976.

Holmvall, M. (2007) *Striping on flexo post-printed corrugated board.* Doctoral dissertation. Mid Sweden University. Available at: https://urn.kb.se/resolve?urn=urn:nbn:se:miun:diva-111 (Accessed: 30 July 2024).

Hunter, S.C. (1961) 'The rolling contact of a rigid cylinder with a viscoelastic half space', *Journal of Applied Mechanics*, 28(4), pp. 611–617. Available at: https://doi.org/10.1115/1.3641792.

Johnson, J., Rättö, P., Lestelius, M. and Blohm, E. (2004) 'Measuring the dynamic pressure in a flexographic central impression printing press', *Nordic Pulp and Paper Research Journal*, 19(1), pp. 84–88. Available at: https://doi.org/10.3183/npprj-2004-19-01-p084-088.

Johnson, M.A. (2003) *Viscoelastic Roll Coating Flows*. Doctoral dissertation. University of Maine. Available at: https://digitalcommons.library.umaine.edu/etd/235/ (Accessed: 11 July 2024).

Kalicinski, S. (2014) *The Effects of Dot Uniformity on Halftone Mottle inFlexographic Prints on Coated Board*. Doctoral dissertation. KTH Royal Institute of Technology. Available at: https://kth.diva-portal.org/smash/record.jsf?pid=diva2%3A743602&dswid=-5334.

Keller, S.F. (1992) 'Measurement of the pressure-time profile in a rolling calender nip' [Preprint].

Kerekes, R.J. (1976) 'Pressure distribution on a thin viscoelastic strip rolling between two rigid cylinders', *Transactions of the Canadian Society for Mechanical Engineering*, 4(1), pp. 27–32. Available at: https://doi.org/10.1139/tcsme-1976-0006.

Khandavalli, S. and Rothstein, J.P. (2017) 'Ink transfer of non-Newtonian fluids from an idealized gravure cell: The effect of shear and extensional deformation', *Journal of Non-Newtonian Fluid Mechanics*, 243, pp. 16–26. Available at: https://doi.org/10.1016/J.JNNFM.2017.02.005.

Lim, C.H., Bohan M.F.J., Claypole, T.C., Gethin, D.T., Roylance, B.J. (1996) 'A finite element investigation into a soft rolling contact supplied by a non-Newtonian ink', *Journal of Physics D: Applied Physics*, 29(7), pp. 1894–1903. Available at: https://doi.org/10.1088/0022-3727/29/7/025.

Litvinov, V. and Farnood, R. (2010) 'Modeling of the compression of coated papers in a soft rolling nip', *Journal of Materials Science*, 45(1), pp. 216–226. Available at: https://doi.org/10.1007/s10853-009-3921-x.

Liu, F. and Shen, W. (2008) 'Forced wetting and dewetting of liquids on solid surfaces and their roles in offset printing', *Colloids and Surfaces A: Physicochemical and Engineering Aspects*, 316(1–3), pp. 62–69. Available at: https://doi.org/10.1016/J.COLSURFA.2007.08.037.

Luong, C.H. and Lindem, P.E. (1997) 'Measurement of the pressure distribution in a soft calender nip', *Nordic Pulp and Paper Research Journal*, 12(3), pp. 207–210. Available at: https://doi.org/10.3183/npprj-1997-12-03-p207-210.

Margetson, J. (1971) 'Rolling contact of a smooth viscoelastic strip between rotating rigid cylinders', *International Journal of Mechanical Sciences*, 13(3), pp. 207–215. Available at: https://doi.org/10.1016/0020-7403(71)90003-8.

Margetson, J. (1972) 'Rolling contact of a rigid cylinder over a smooth elastic or viscoelastic layer', *Acta Mechanica*, 13(1–2), pp. 1–9. Available at: https://doi.org/10.1007/BF01179654.

Morgan, M.L., Holder, A., Curtis, D.J., Deganello, D. (2018) 'Formulation, characterisation and flexographic printing of novel Boger fluids to assess the effects of ink elasticity on print uniformity', *Rheologica Acta*, 57(2), pp. 105–112. Available at: https://doi.org/10.1007/S00397-017-1061-9.

Schultz-Eklund, O., Fellers, C. and Johansson, P.-Å. (1992) 'Method for the local determination of the thickness and density of paper', *Nordic Pulp and Paper Research Journal*, 7(3), pp. 133–139. Available at: https://doi.org/10.3183/npprj-1992-07-03-p133-139.

Tollenaar, D. and Ernst, P.A.H. (1961) 'Optical density and ink layer thickness', in Banks, W.H. (ed.) *Advances in Printing Science and Technology. Vol. 2: Problems in High Speed Printing.* Oxford: Pergamon Press, pp. 214–228. Available at: https://cir.nii.ac.jp/crid/1572824499849480704 (Accessed: 18 July 2024).

Wang, G. and Knothe, K. (1993) 'Stress analysis for rolling contact between two viscoelastic cylinders', *Journal of Applied Mechanics*, 60(2), pp. 310–317. Available at: https://doi.org/10.1115/1.2900794.

Watanabe, K. and Amari, T. (1982) 'Dynamic compressive modulus of paper', *Reports on Progress in Polymer Physics in Japan*, XXV, pp. 409–412.

Wu, J.T., Carvalho, M.S. and Kumar, S. (2019) 'Effects of shear and extensional rheology on liquid transfer between two flat surfaces', *Journal of Non-Newtonian Fluid Mechanics*, 274, 104173. Available at: https://doi.org/10.1016/J.JNNFM.2019.104173.

Xue, Y.K., Gethin, D.T. and Lim, C.H. (1994) 'Numerical modelling of the contact between lithographic printing press rollers by soft EHL theory', *Proceedings of the Institution of Mechanical Engineers, Part C: Journal of Mechanical Engineering Science*, 208(5), pp. 381–390. Available at: https://doi.org/10.1243/PIME_PROC_1994_208_381_02.

Yoneyama, S., Gotoh, J. and Takashi, M. (2000) 'Experimental analysis of rolling contact stresses in a viscoelastic strip', *Experimental Mechanics*, 40(2), pp. 203–210. Available at: https://doi.org/10.1007/BF02325047.